

# CausalSpatial: A Benchmark for Object-Centric Causal Spatial Reasoning

Wenxin Ma <sup>\*1,2</sup> Chenlong Wang <sup>\*1</sup> Ruisheng Yuan <sup>\*1</sup> Hao Chen <sup>1</sup> Nanru Dai <sup>1</sup> S. Kevin Zhou <sup>2</sup> Yijun Yang <sup>3</sup>  
Alan Yuille <sup>1</sup> Jieneng Chen <sup>1</sup>

## Abstract

Humans can look at a static scene and instantly predict what happens next — *will moving this object cause a collision?* We call this ability Causal Spatial Reasoning. However, current multimodal large language models (MLLMs) cannot do this, as they remain largely restricted to static spatial perception, struggling to answer “what-if” questions in a 3D scene. We introduce **CausalSpatial**, a diagnostic benchmark evaluating whether models can anticipate consequences of object motions across four tasks: Collision, Compatibility, Occlusion, and Trajectory. Results expose a severe gap: humans score 84% while GPT-5 achieves only 54%. Why do MLLMs fail? Our analysis uncovers a fundamental deficiency: models over-rely on textual chain-of-thought reasoning that drifts from visual evidence, producing fluent but spatially ungrounded hallucinations. To address this, we propose the **CAUSAL OBJECT WORLD MODEL** (COW), a framework that externalizes the simulation process by generating videos of hypothetical dynamics. With explicit visual cues of causality, COW enables models to ground their reasoning in physical reality rather than linguistic priors. We make the dataset and code publicly available: <https://github.com/CausalSpatial/CausalSpatial>.

## 1. Introduction

Humans can naturally perceive their surroundings and form a mental 3D model of the world. This mental model enables us to simulate possible physical interactions between objects in space. For example, as shown in Figure 1, in a static scene where a car faces a metal vase, we can use spatial cues such as proximity and orientation to predict a potential

<sup>1</sup>Johns Hopkins University <sup>2</sup>USTC <sup>3</sup>HKUST. Correspondence to: Jieneng Chen <jchen293@jh.edu>.

Preprint. January 21, 2026.

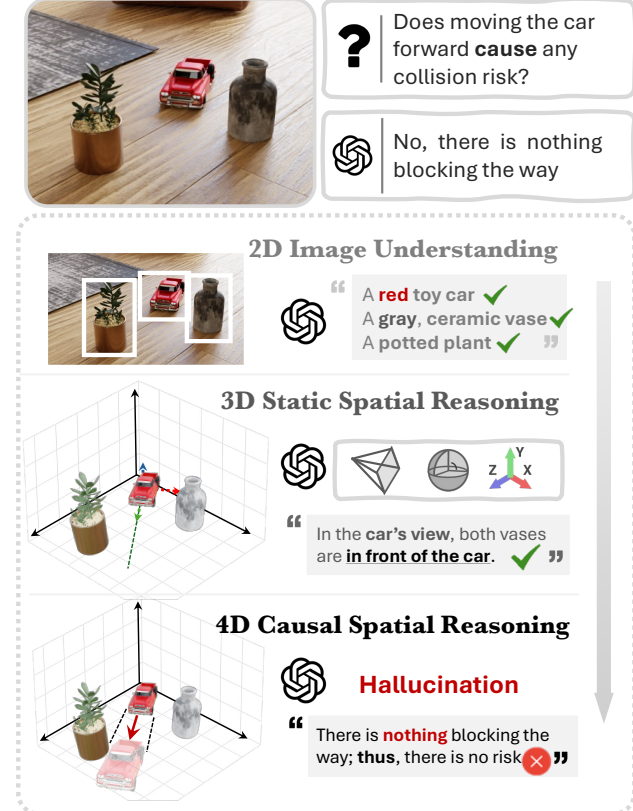


**Figure 1. Causal spatial reasoning task.** The task requires model to progress from 2D image understanding to 3D spatial perception and ultimately to 4D causal spatial reasoning—predicting how actions affect future spatial configurations. Current MLLMs fail at this complex task due to hallucinations.

collision if the car moves forward. We refer to this task of grounding causal inference in spatial reasoning as **Causal Spatial Reasoning**.

This task requires three progressive spatial reasoning capabilities. As illustrated in Figure 1, the process begins with 2D image understanding and 3D static spatial reasoning. In these paradigms, models are tasked with recognizing objects and estimating spatial cues, such as camera perspective, orientation, and distance. While these capabilities form the foundation for further reasoning, they are inherently

Benchmark	Evaluation				Design	
	2D	3D	TD	CP	OM	RL
CLEVR-Count (Johnson et al., 2017b)	✓					
CLEVR (Johnson et al., 2017a)	✓					
VQA (Goyal et al., 2017)	✓				✓	
GQA (Hudson & Manning, 2019a)	✓				✓	
CV-Bench (Tong et al., 2024a)	✓	✓			✓	
SAT (Ray et al., 2024)	✓	✓	✓		✓	
STI-Bench (Li et al., 2025)	✓	✓	✓		✓	
Spatial457 (L1-4) (Wang et al., 2025c)	✓	✓		✓		
CausalVQA (Foss et al., 2025)	✓		✓	✓		✓
VSI-Super (Yang et al., 2025)	✓	✓	✓			✓
<b>CausalSpatial</b>	✓	✓	✓	✓	✓	✓

*Table 1. Comparison of benchmarks.* **2D** denotes *2D perception*; **3D** denotes *3D static relation*; **TD** denotes *Temporal Dynamics*; **CP** denotes *Causal Prediction*. **OM** denotes *Object-level Manipulation*. **RL** denotes *Realistic*. CausalSpatial involves diverse paradigms of spatial reasoning, spanning from 2D perception to temporal dynamics. It incorporates causal prediction into spatial reasoning, paving the way for the next-level vision intelligence. Complete table is available in Appendix B.

*static*—answering only “what/where is something” but failing to address “what will happen if...”, which is critical for understanding the physical world. To reason about causality, models must advance to 4D causal spatial reasoning, a comprehensive and dynamic paradigm that integrates spatial understanding with temporal prediction. Rather than analyzing spatial cues in isolation, models must synthesize this information to form coherent mental simulations. This requires first extracting 3D spatial relationships from static images, then simulating hypothetical or counterfactual interactions with temporal consistency (e.g., “The car will collide with the vase if it moves forward.”).

While humans perform causal spatial reasoning effortlessly, whether MLLMs possess this capability remains largely underexplored. Current evaluation frameworks (as listed in Table 1) are limited to *2D* and *3D* static reasoning or overlook object interactions, failing to assess whether models can reason about how objects dynamically affect each other in the given spatial contexts.

To fill this gap, we propose CausalSpatial, a synthetic benchmark designed to diagnose causal spatial reasoning capabilities from an object-centric perspective. Each evaluation item consists of an image showing multiple objects in a scene, paired with a hypothetical object-level motion context (e.g., If the car moves forward, a collision may occur.). This setup requires the model to move beyond static recognition of the given static image, and simulate the future object interaction outcomes according to the motion context. To provide a comprehensive diagnosis, we define four distinct forms of causal anticipation under different spatial configurations: ***Collision***, ***Occlusion***, ***Compatibility***, and ***Trajectory***. As the first open-source diagnostic

benchmark of its kind, CausalSpatial provides the necessary testbed for advancing models toward more robust and causally grounded spatial understanding.

Extensive experiments on CausalSpatial expose a critical disparity between state-of-the-art MLLMs and human capabilities. Our analysis attributes this failure to a fundamental deficiency: with recent improvements in reasoning capability, MLLMs typically over-rely on a textual Chain-of-Thought (CoT) to infer dynamics and reason about causality. However, such textual CoT struggles to maintain consistent alignment with the original visual input, resulting in inaccurate spatial information during reasoning. Consequently, subsequent textual causal reasoning often includes spatial illusion, making models to generate seemingly plausible yet spatially ungrounded predictions.

To address the failure of text-based causal reasoning in maintaining spatial grounding, we propose leveraging world models to provide explicit causality hints with consistent 4D trajectory control. We propose **CAUSAL OBJECT WORLD MODEL** (COW), an object-centric world model that externalizes the simulation process by rendering hypothetical object dynamics into video. Unlike textual reasoning, which drifts from reality, COW generates realistic future frames based on extracted 4D trajectories. This explicit visual evidence effectively compensates for the models’ inability to perform internal physical simulation, enabling grounded causal inference and demonstrating significant promise in complex spatial reasoning tasks.

In summary, our contribution is three-fold:

- We introduce CausalSpatial, the first object-centric causal spatial reasoning benchmark, comprising diverse causal spatial scenarios. It provides a comprehensive and diagnostic testbed for causal spatial reasoning.
- We conduct extensive experiments on CausalSpatial across a diverse set of MLLMs, revealing a significant performance gap between machines and humans. Our analysis indicates that models hallucinate in textual CoT, struggling to conduct consistent causal reasoning anchored to actual 3D configurations.
- We propose **CAUSAL OBJECT WORLD MODEL**, an object-centric video generation framework that maintains 3D consistency by fusing spatial cues and simulates cause-and-effect dynamics via rendering videos, paving the way for leveraging WMs in advanced causal spatial reasoning in MLLMs.

## 2. CausalSpatial Benchmark

In this section, we formally present CausalSpatial, a diagnostic benchmark designed to assess the capability of MLLMs in grounding causal inference within 3D spatial environments. We begin by formulating the question of

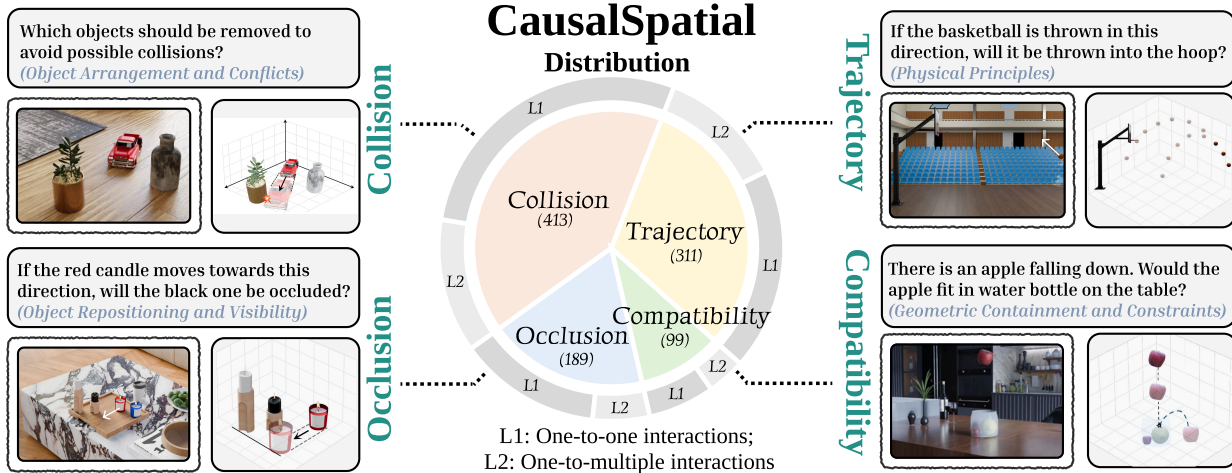


**Figure 2. CausalSpatial tasks.** CausalSpatial encompasses four causal reasoning tasks that require models to anticipate physical outcomes in 3D scenes: Collision, Occlusion, Trajectory, and Compatibility. The number of evaluation entries for each task is listed in the middle. Each task is designed with two difficulty levels, denoted as “L1/L2”. All scenes are rendered in Blender to provide realistic 3D environments for physics-grounded evaluation.

causal spatial reasoning (Section 2.1), followed by a detailed taxonomy of the four proposed subtasks (Section 2.2). We then describe our data collection and annotation pipeline (Section 2.3) and conclude with a comprehensive evaluation of current state-of-the-art models (Section 2.4).

## 2.1. Benchmark Design

The design of CausalSpatial aims to provide a diagnostic assessment of MLLMs’ causal spatial reasoning capabilities. We simplify the analysis by focusing on scenarios where one object moves hypothetically, and examine how this motion might subsequently affect other objects in the scene. We formalize each scenario as a state-transition problem: given an initial scene configuration, the model must predict the outcome when a specific object undergoes motion. Each query explicitly identifies the moving object to ensure the model performs object-grounded spatial reasoning rather than superficial pattern matching.

**Question formulation.** Each query in CausalSpatial consists of an image  $I_0$  which captures a 3D scene and a textual motion context  $T$  describing a hypothetical motion. The input image  $I_0$  is captured at the initial state  $S_0$ . The model is tasked by predicting the future spatial states  $S$  after the hypothetical motion. Unlike traditional VQA, which queries existing static attributes in an image, this task requires the model to approximate a transition function  $f : S_0 | I_0, m \rightarrow S_{future}$ , simulating the dynamic evolution of the scene solely based on visual spatial information and internalized physical world.

**Object-level design.** A key feature of CausalSpatial is the object-level nature. In CausalSpatial, each motion context focuses on a specific target object and its potential

interaction with the surrounding environment. This setup decouples complex scene dynamics into manageable interaction units, requiring the model to: (1) perceive the precise 3D spatial attributes of objects in the image (*e.g.*, position, orientation, geometry); (2) perform a mental simulation of the hypothetical motion  $m$ ; and (3) reason about the causal consequences (*e.g.*, collision, occlusion) resulting from the interaction between the target and other objects.

## 2.2. Taxonomy

To systematically evaluate the causal spatial reasoning capability, as shown in Figure 2, we design four types of hypothetical anticipation tasks. Each task reflects a distinct aspect of causal spatial ability.

**Collision anticipation** evaluates the capability to reason about *object arrangement and conflicts*. In this task, models must predict: (1) whether a collision would occur if a target object moves forward, and (2) whether the collision outcome would change if another specific object were removed from the scene. Successfully addressing this task demands precise recognition of the spatial attributes of the target object (*e.g.*, orientation, size), and the spatial relationship among different objects (*e.g.*, distance, relative position).

**Occlusion anticipation** evaluates the capability to reason about *how object repositioning alters the visible scene structure*. In this task, objects are arranged in a 3D scene with complex depth relationships. Models must predict how moving a target object affects the visibility of other objects. Success requires understanding the camera perspective, analyzing spatial occlusion relationships between objects, and predicting how spatial adjustments affect visibility.

**Trajectory anticipation** evaluates the ability to predict object motion under *physical principles and causal constraints*. In this task, target objects move according to basic physical laws such as gravity, bouncing, and momentum transfer. Models must predict how objects interact with the environment or other objects (e.g., whether a moving billiard ball will collide with others and where it will travel).

**Compatibility anticipation** evaluates the capability to reason about *geometric containment and spatial constraints*. In this task, models are given a hypothetical placement (e.g., “If I want to put an apple into the bowl...”), and are required to assess containment feasibility. Specifically, models must determine whether issues such as overflow, spatial overlap, geometric penetration, or physical instability would occur. Success requires fine-grained understanding of object geometry, including size, shape, and volume relationships.

**Two levels of difficulty.** For each category, we define two difficulty levels: **(L1) One-to-one reasoning**, which focuses on reasoning about interactions between a single pair of objects, and **(L2) One-to-multiple reasoning**, which requires comprehending how a target object simultaneously relates to multiple others within the scene. This hierarchical formulation enables systematic evaluation of both basic pairwise reasoning and the model’s ability to generalize towards more complex, compositional multi-object interactions.

### 2.3. Data Collection and Annotation

To comprehensively evaluate the causal spatial reasoning capabilities of MLLMs, we construct CausalSpatial using publicly available realistic 3D scenes and assets. Specifically, we curate a diverse collection of 3D object assets spanning over 50 object categories. To ensure visual realism and diversity, we manually refine the texture of each object asset. Each scene is accompanied by thorough annotations, including RGB images, depth maps, and oriented bounding boxes, which enable accurate question generation.

For each scene, we design multiple action prompts that specify hypothetical or counterfactual object motions. These motion events are physically simulated and rendered using Blender’s physics engine, ensuring all outcomes adhere to real-world dynamics and physical plausibility. Each evaluation instance undergoes rigorous human verification to ensure causal correctness and quality. Full construction details are provided in the Appendix C.

### 2.4. Benchmarking

In this section, we detail the experiment setup (Section 2.4.1) and then report quantitative results and key observations on CausalSpatial (Section 2.4.2). We discuss failure cases and possible improve directions in Section 2.4.3. Our analysis highlights the substantial gap between current MLLMs and

human intelligence.

#### 2.4.1. EVALUATION SETUP

**Evaluated MLLMs.** Our evaluation spans a diverse set of state-of-the-art MLLMs, including powerful open-source models (Spatial-VLM(Chen et al., 2024), Spatial-MLLM(Wu et al., 2025a), and the Qwen-VL series(Team, 2025c; Bai et al., 2025)) as well as leading closed-source MLLMs (GPT-5 series(OpenAI, 2025a), Gemini 2.5 series(Team, 2025b), and Claude(Anthropic, 2025)). These models represent the cutting edge of spatial reasoning, providing a robust baseline for assessing current capabilities in causal spatial reasoning. Additionally, to establish a human performance reference, we recruited three independent evaluators to complete the CausalSpatial benchmark. We also report random guessing scores to contextualize the difficulty of the tasks and better reflect model capabilities.

**Metrics.** Standard binary evaluation paradigms often incentivize hallucinations by rewarding forced guessing over acknowledging uncertainty (OpenAI, 2025c). In spatial reasoning, there exists an inherent ambiguity in complex spatial dynamics, triggering the hallucination of MLLMs. To mitigate this bias and better analyze whether models can distinguish knowns from unknowns, we explicitly introduce a “Not Sure” option, allowing models to abstain when uncertain. Accordingly, we adopt two complementary metrics: (1) **True Positive Rate (TPR)**, which measures the proportion of correctly answered questions among all samples, reflecting the model’s grounded reasoning accuracy; and (2) **Not Sure Rate (NSR)**, which quantifies the proportion of responses where the model chooses “Not Sure” option. This dual-metric setup allows us to decouple confident errors (hallucinations) from epistemic uncertainty, providing a clearer view of the model’s behavioral calibration.

**Evaluation details.** The evaluation items in CausalSpatial are formatted as multiple-choice questions. We prompt the models to reason over the question and put their answer in the {“Reasoning”:..., “Answer”:...} JSON format. The maximum output length is set to 8192 tokens to allow for complete reasoning traces. Each question is evaluated five times to ensure robustness and reduce randomness. Full details and analysis are presented in Appendix D.

#### 2.4.2. BENCHMARK ANALYSIS

**Main results.** The results demonstrate a critical disparity between MLLMs and humans. As detailed in Table 2, humans maintain high accuracy across Level 1 (85.44%) and Level 2 (83.54%). However, MLLMs struggle to bridge this gap. Even the state-of-the-art GPT5 only achieves 54.17%, indicating causal spatial reasoning remains a significant challenge for current models.

Model	Level 1						Level 2						Avg.	Rank
	Col.	Com.	Occ.	Traj.	Avg.	Col.	Com.	Occ.	Traj.	Avg.	Col.	Com.		
<b>Spatial Reasoning MLLMs</b>														
Spatial-VLM(Chen et al., 2024)	20.98	47.62	48.15	46.88	36.24 (3.83)	15.75	41.67	24.07	37.96	28.25 (7.17)	33.50	15		
Spatial-MLLM(Wu et al., 2025a)	41.96	55.56	48.15	54.17	47.93 (1.91)	24.41	44.44	12.96	24.82	24.56 (0.72)	40.00	12		
<b>Open-source MLLMs</b>														
LLaVAOneVision1.5-8B-I. (Li et al., 2024)	43.01	42.86	38.52	29.17	38.17 (15.91)	15.38	41.67	20.37	38.69	27.84 (23.30)	34.62	14		
Qwen2.5-VL-7B-I.(Team, 2025c)	41.75	42.86	42.22	44.27	42.66 (2.21)	30.40	41.67	24.07	38.69	33.79 (5.73)	39.61	13		
Qwen3-VL-2B-I.(Team, 2025c)	47.43	47.62	49.63	43.23	46.69 (0.88)	19.35	38.89	22.22	37.96	28.98 (1.79)	40.60	11		
Qwen3-VL-4B-I.(Team, 2025c)	47.55	50.79	48.15	44.79	47.19 (6.92)	24.41	44.44	16.67	62.77	40.11 (10.39)	44.76	8		
Qwen3-VL-8B-I.(Team, 2025c)	41.40	66.67	51.11	47.92	47.55 (2.95)	22.76	36.11	29.63	50.36	35.85 (7.89)	43.53	9		
Qwen3-VL-8B-T.(Team, 2025c)	42.74	63.49	48.15	55.73	49.43 (1.03)	23.75	44.44	22.22	34.31	29.71 (1.79)	42.65	10		
Qwen3-VL-30B-A3B-I.(Team, 2025c)	47.02	55.56	48.15	47.40	48.15 (1.47)	30.16	52.78	31.48	52.55	41.32 (1.08)	45.80	6		
Qwen3-VL-30B-A3B-T.(Team, 2025c)	52.99	58.73	51.11	54.17	53.49 (0.00)	35.09	63.89	46.30	48.18	44.79 (0.36)	50.50	3		
<b>Closed-source MLLMs</b>														
GPT5(OpenAI, 2025a)	49.65	61.90	59.26	54.17	54.00 (1.47)	40.94	50.00	62.96	64.96	54.52 (1.08)	54.17	1		
GPT5-mini(OpenAI, 2025a)	37.76	42.86	48.15	44.79	42.31 (6.19)	35.43	47.22	50.00	67.88	51.41 (3.94)	45.44	7		
Gemini2.5 Pro(Team, 2025a)	43.62	63.49	60.00	53.12	51.44 (0.00)	30.65	52.78	48.15	64.96	48.85 (0.36)	50.55	2		
Gemini2.5 Flash(Team, 2025b)	46.21	50.79	48.89	56.25	50.02 (0.15)	42.31	58.33	25.93	55.47	46.53 (1.79)	48.82	4		
Sonnet 3.7(Anthropic, 2025)	55.00	49.21	45.56	46.35	50.12 (5.04)	29.41	48.61	34.26	60.58	44.16 (17.29)	48.07	5		
Human	86.84	80.00	92.50	82.50	85.44	78.57	97.22	97.50	62.50	83.54	84.49	-		
Random	23.61	31.75	32.35	38.54	30.34	8.54	33.33	20.37	32.14	24.50	28.6	-		

**Table 2. The performance of MLLMs on CausalSpatial.** *Col.* denotes Collision anticipation. *Com.* denotes Compatibility anticipation. *Occ.* denotes Occlusion anticipation. *Traj.* denotes Trajectory anticipation. *Avg.* denotes Average scores. Best & Second best. The gray figures denote the Not Sure Rate (NSR) defined in §2.4.1. A clear performance gap between human and MLLMs.

In the open-source landscape, the Qwen3-VL series demonstrates superior efficiency. Qwen3-VL-30B-A3B-T shows the best performance (53.49% on Level 1 and 50.50% on Level 2), narrowing the gap with closed-source MLLMs. The compact Qwen3-VL-2B-I notably outperforms significantly larger models from other families, such as Qwen2.5-VL-7B (39.61%) and LLaVA-OneVision-8B (34.62%). Furthermore, specialized spatial reasoning MLLMs generally underperform compared to general-purpose MLLMs, highlighting the unique difficulty of our causal spatial tasks.

**Different reasoning subtasks.** Performance varies significantly across subtasks, with Collision Anticipation emerging as the most challenging category for MLLMs. While human participants maintain high accuracy (78.57%) even in complex Level 2 scenarios, most models suffer a severe performance collapse, with open-source models like LLaVA-OneVision falling to 15.38%, modestly surpassing the random guessing.

Occlusion Anticipation further differentiates model capabilities. While open-source models generally struggle with dynamic occlusion in Level 2 (hovering around 20-30%), closed-source frontier models like GPT-5 demonstrate superior robustness (62.96%), suggesting a stronger internal representation of 3D spatial structures.

In contrast, the Trajectory task exhibits a unique trend where the performance gap between MLLMs and humans is narrowest. MLLMs demonstrate surprising competence in Trajectory task, with some models approaching human-level

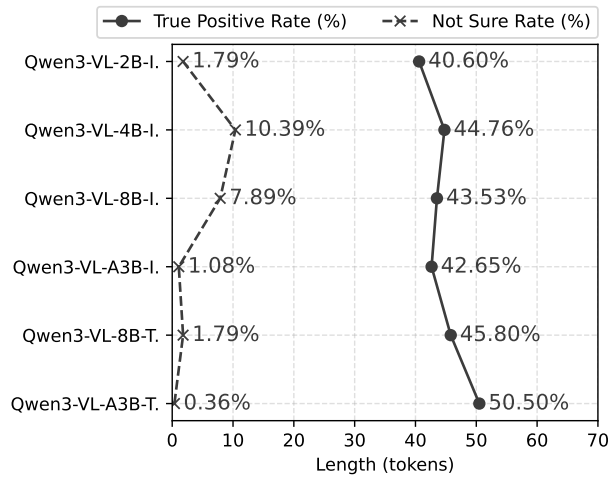


**Figure 3. Statistics for output length (token), True Positive Rate, and Not Sure Rate.** The comparison emphasizes limited returns from model scaling on causal spatial reasoning, while larger models exhibit significantly lower NSR.

accuracy (62.50% on Level 2 for humans and 64.96% on Level 2 for GPT 5). This suggests that while models lack the grounded understanding required for complex interaction dynamics like collisions, they are relatively effective at patterns like matching trajectory paths. Conversely, that human intuition for precise trajectory prediction is inherently less reliable than their semantic understanding.

**Different model sizes.** As detailed in Figure 3, we observe limited returns from model scaling within the Qwen3-VL

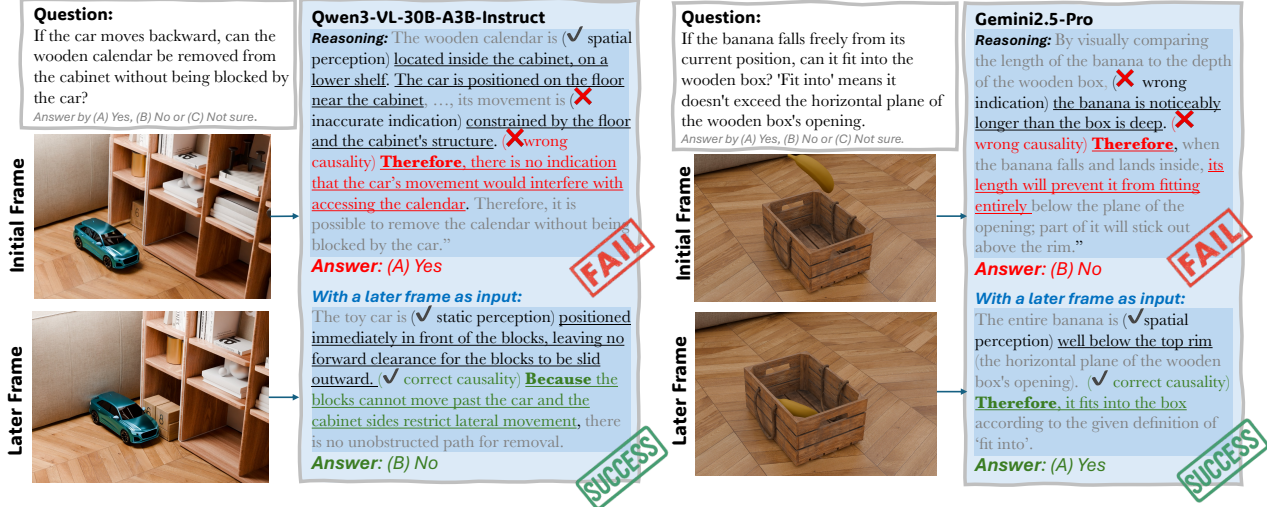


**Figure 4. Why do SoTA MLLMs fail in CausalSpatial?** These examples illustrate how MLLMs often produce lengthy and seemingly coherent explanations while failing to ground their reasoning in the visual evidence. In the car–cabinet scenario (*Left*), the model ignores the visible placement of the toy car directly blocking the wooden calendar and instead follows a generic linguistic pattern about object removal. In the banana–box example (*Right*), the model asserts that the banana exceeds the box depth—an inference inconsistent with the image. Across such failure modes, the reasoning chains are verbose but inaccurate, revealing that current MLLMs fail to simulate the motion process by solely relying on the textual reasoning.

series. The instruction-tuned variants exhibit performance plateaus, with the 4B, 8B, and 30B-A3B models achieving similar scores of 44.76%, 43.53%, and 45.80%, respectively. This saturation reveals that model size scaling, though effective for general tasks, does not directly translate to improvements in causal spatial reasoning.

At the same time, we observe a decoupling between model confidence and accuracy performance. Larger models become increasingly decisive, often unwarranted. As shown in Figure 3, scaling model parameters dramatically reduces uncertainty. The Not Sure Rate (NSR) falls from 18.77% on Qwen3-4B-I to nearly zero (0.10%) on Qwen3-30B-A3B-T. This trend is further exacerbated by the thinking mode, where the NSR drops even more aggressively (*e.g.*, from 10.57% (I) to 2.37% (T) on Qwen3-8B, from 2.84% (I) to 0.10% (T) on Qwen3-30B-A3B). However, this decisiveness is deceptive. The sharp decrease in uncertainty is not accompanied by a corresponding leap in accuracy.

#### 2.4.3. FAILURE ANALYSIS & IMPROVE DIRECTIONS

Despite the challenging nature of causal spatial reasoning revealed by our benchmark, understanding *why* current MLLMs fail and *how* to address these failures provides valuable insights for future progress. We conduct a detailed failure analysis and discuss promising directions for improvement in this section.

**Why do SoTA MLLMs fail in CausalSpatial?** Figure 4 illustrates representative failure cases from Qwen3-VL-30B-

A3B-Instruct (Team, 2025c) and Gemini2.5-Pro (Team, 2025a). Initially, MLLMs generally succeed at identifying static object positions and spatial relationships. However, a critical disconnect occurs during the subsequent reasoning phase. These visual cues are either diluted or misinterpreted as the textual chain progresses. In the car–cabinet example, the model produces a coherent explanation but does not consider the car’s visible position in front of the wooden calendar, resulting in an incorrect answer. In the banana–box example, the model concludes that the banana is longer than the depth of the box, which is not supported by the image.

Consistent with prior studies (Chen et al., 2025; OpenAI, 2025c), we observe that MLLMs prefer to reason based on linguistic priors rather than grounding their logic in the image. Consequently, when conducting causal spatial reasoning, models tend to drift toward generic textual CoT, which includes remarkable hallucinations, neglecting the specific geometric constraints present in the visual input.

This analysis reveals a critical challenge: *MLLMs fail to ground their reasoning in the geometry evidence, drifting toward linguistically plausible but spatially inaccurate explanations with inaccurate prediction.*

**How to anchor reasoning in 3D constraints?** World Models (WMs) offer a promising solution, as they are fundamentally designed to capture causal outcomes and temporally consistent dynamics given hypothetical actions. However, existing world models (Lu et al., 2025; Wan et al., 2025) are limited to scene exploration, primarily generating static

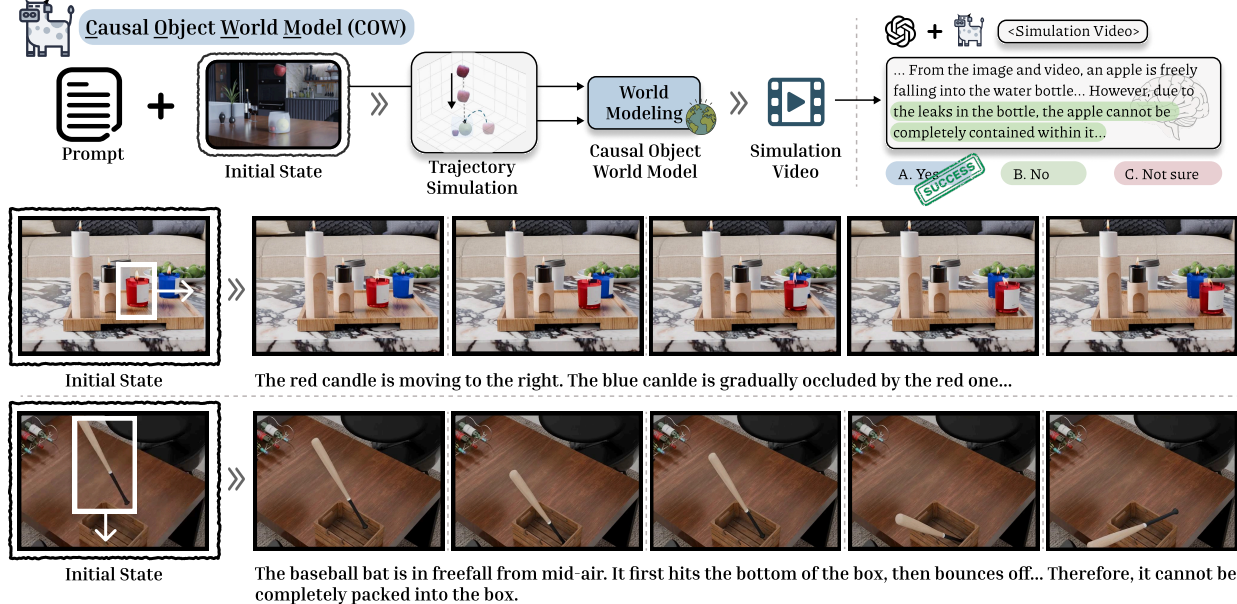


**Figure 5. (A) COW pipeline overview:** COW is a 4D trajectory-controlled video generation method that enhances spatial reasoning by explicitly rendering object dynamics through object-centric video generation. **(B) Qualitative results:** COW produces physically and visually plausible simulation videos that offer clear visual cues for improved causal spatial inference.

environments with moving viewpoints, and thus overlook object-level spatial consistency critical for causal reasoning. Accordingly, we argue that a world model maintaining strict object-level spatial consistency can serve as a reliable visual grounding mechanism, enabling MLLMs to perform accurate causal spatial reasoning.

### 3. COW: CAUSAL OBJECT WORLD MODEL

Based on above discussions, we propose our implementation of **CAUSAL OBJECT WORLD MODEL**, a framework designed for fine-grained control over 4D object trajectories. By synthesizing physically plausible video sequences based on the trajectories, our approach effectively grounds MLLMs in actual 3D scene. The pipeline design is described in Section 3.1. We evaluate the effectiveness on CausalSpatial and discuss the future direction in Section 3.2. Further details are available in Appendix F.

#### 3.1. COW Pipeline

The queries from CausalSpatial consist of an image representing the initial state and a motion context implying an intervention. COW processes this information, externalizes causality modeling by trajectory simulation and trajectory-conditioned video generation, providing rich visual cues for the MLLMs reasoning. The pipeline of COW includes three key steps.

**4D trajectory simulation.** We extend the spatial state into a 4D representation using a 6-dimensional vector  $Obj_i = \{x, y, z, v_x, v_y, v_z\}$ . The initial position  $\{(x, y, z)\}$  (predict

the bounding box) and  $\vec{v} = \{v_x, v_y, v_z\}$  (predict the object orientation or direction indicator in images) are estimated via prompting MLLMs. We then construct the synthetic trajectory  $\tau$  by iteratively updating the object’s position, modulated by external physical factors, such as gravity.

**Controllable video generation.** We employ ATI (Wang et al., 2025a) as the world model to render physically consistent dynamics. The predicted trajectories  $\tau_i$  and motion descriptions  $m_i$  serve as control signals to condition a diffusion-based generator, synthesizing coherent frames:  $F_{later} = \mathcal{W}_\theta(F_{init} | \tau_i^t, d_i)$ . This design leverages the rich priors of large-scale video models, effectively bridging analytical physical modeling with data-driven imagination for realistic simulation.

**Assist MLLMs in reasoning.** We integrate COW with an MLLM to enable temporally grounded reasoning. The MLLM jointly interprets the simulated video and the text query to generate informed answers, effectively moving beyond static perception to support motion process prediction.

#### 3.2. Evaluate COW

**Experiment setup** We use the three initial frames from generated videos as additional visual cues for subsequent reasoning. All images are resized to 512 pixels. We test the representative model, Qwen3-VL-30B-A3B-Instruct, to evaluate the effectiveness of COW. Experiments are repeated three times to ensure robustness.

**Main results.** Figure 6 demonstrates a consistent performance boost on CausalSpatial. Introducing merely three

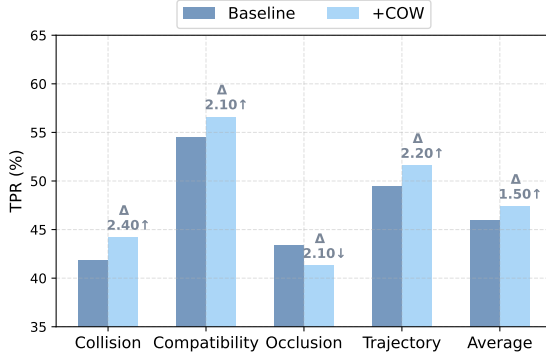


**Figure 6. Quantitative results of COW.** The visual simulation leads to considerable performance gains in CausalSpatial, highlighting the potential of explicit vision simulation.

frames from the generated video yields a notable accuracy improvement, 2.40% on Collision and 2.20% on Trajectory. Crucially, COW only provides a limited number of simulated frames to MLLMs, which can already improve the model’s performance in spatial reasoning without requiring extra training or datasets. These results validate the effectiveness of visual simulation.

However, there is a slight decrease in the Occlusion task. A possible reason lies in the continuous nature of the Occlusion task (e.g., The target object may be occluded during the initial stages, yet eventually revealed in later frames.) Since the first few video frames only simulate the immediate future, they provide limited visual cues for subsequent long-term reasoning required by MLLMs.

### 3.3. Discussion

As illustrated in Figure 4, the additional simulated images play a pivotal role in anchoring the initial state implied by the question image, thus facilitating reasoning about the subsequent dynamics. In the car-cabinet example, the model correctly interprets the spatial arrangement, identifying the visible blocking between the car and wooden cabinet. Similarly, in the banana-box example, COW successfully simulates the future state where the banana lies in the box, enabling the model to accurately assess their size relationship and avoid the previous erroneous conclusion about depth incompatibility. These cases demonstrate a clear pattern: when equipped with simulated future states, the model effectively suppresses hallucinations by grounding its reasoning in accurate visual dynamics rather than unreliable linguistic priors. This visual grounding mechanism proves crucial for maintaining reasoning accuracy.

Consequently, the quality and physical plausibility of generated videos are critical to reasoning accuracy. COW maintains precise geometric consistency by grounding video generation in explicit object trajectories, ensuring that simulated dynamics remain spatially coherent throughout the temporal

sequence. However, how to guarantee this consistency in additional geometric attributes such as volume, shape deformation, and inter-object collision dynamics remains an open question for future works.

## 4. Related Work

**Causal spatial reasoning.** Recent multimodal advances have empowered spatial reasoning (Cheng et al., 2024; Ray et al., 2024; Chen et al., 2024; Wu et al., 2025a; Team, 2025c;b; Lian et al., 2025; Tang et al., 2024). However, existing benchmarks largely remain at the perceptual and simple understanding level. Early datasets (Johnson et al., 2017c; Li et al., 2023; Hudson & Manning, 2019b; Tong et al., 2024b; Liu et al., 2023; Ma et al., 2025) focus on *static 3D relations*, while dynamic 4D benchmarks (Li et al., 2025; Zhou et al., 2025b;a; Parmar et al., 2025; Lin et al., 2025) introduce temporal cues but are limited to *passive motion tracking*. Recent studies (Wang et al., 2025c; Qi et al., 2025; Liu et al., 2025; Wu et al., 2025b) make more comprehensive efforts, attempting to unify these aspects, yet rely on unrealistic scenes that lack physical fidelity. Crucially, true spatial intelligence demands ***causal reasoning***, not just observing “what/where is something”, but predicting “what will happen”. To this end, we propose CausalSpatial. Unlike prior works restricted to descriptive tasks, CausalSpatial emphasizes causal prediction from object-level manipulations, requiring MLLMs to mentally simulate consistent physical dynamics to infer future outcomes.

**Video Generation & World Models.** World models (Ha & Schmidhuber, 2018; Wan et al., 2025; Wang et al., 2025b; Lu et al., 2025; Wang et al., 2025a; Cui et al., 2025; Guo et al., 2025; OpenAI, 2025b; Deepmind, 2025) have shown remarkable success in robotics (Zhen et al., 2024; Zhou et al., 2024; Ling et al., 2025; Zhang et al., 2024; Long et al., 2025) and autonomous driving (Hu et al., 2023; Gao et al., 2024; Koh et al., 2021), acting as dynamic simulators for anticipation and decision-making (LeCun, 2022; Seo et al., 2023; Hafner et al., 2021; Parker-Holder et al., 2024; Yu et al., 2025a; Wu et al., 2023a). However, existing models predominantly focus on global scene dynamics (Alonso et al., 2024; Yu et al., 2025b) or ego-motion (Du et al., 2023; Ko et al., 2023; Yang et al., 2023; Zhen et al., 2025), often lacking the granularity to manipulate specific objects within the scene. This limitation restricts their utility in complex scenarios where precise object-level interaction is essential. While recent work has explored object-centric representations (Wu et al., 2023b; Locatello et al., 2020; Didolkar et al., 2025), these approaches primarily focus on synthetic scenes or image generation and do not extend to the complex physical reasoning required for causal spatial tasks. To bridge this gap, we introduce **Causal Object World Model (COW)**. Unlike holistic scene

predictors, COW is an object-centric pipeline specifically targets on trajectory-controlled object motion control, enabling the precise simulation of interactions required for rigorous causal reasoning.

## 5. Conclusion

In this paper, we define a higher-level spatial reasoning paradigm, Causal Spatial Reasoning, a significant step to bridge the virtual reasoning and the physical world. To better investigate this question, we present CausalSpatial, the first-of-this-kind benchmark designed to evaluate causal spatial reasoning capabilities. Extensive experiments reveal that current models struggle to form coherent mental simulations for advanced reasoning. To address this, we introduced COW, a world-model-based framework that generates controllable object-level motion simulation to support temporally grounded reasoning. The experimental improvements highlight the importance of explicit causal imaginations in modeling causal processes, pointing the direction for future exploration.

## References

Alonso, E., Jolley, A., Michel, V., Kanervisto, A., Storkey, A. J., Pearce, T., and Fleuret, F. Diffusion for world modeling: Visual details matter in atari. *NeurIPS*, 2024.

Anthropic. Claude sonnet 3.7, 2025. URL <https://www.anthropic.com/news/clause-3-7-sonnet>.

Bai, S., Chen, K., Liu, X., Wang, J., Ge, W., Song, S., Dang, K., Wang, P., Wang, S., Tang, J., et al. Qwen2. 5-vl technical report. *arXiv preprint arXiv:2502.13923*, 2025.

Chen, B., Xu, Z., Kirmani, S., Ichter, B., Sadigh, D., Guibas, L., and Xia, F. Spatialvlm: Endowing vision-language models with spatial reasoning capabilities. In *CVPR*, pp. 14455–14465, 2024.

Chen, S., Zhu, T., Zhou, R., Zhang, J., Gao, S., Niebles, J. C., Geva, M., He, J., Wu, J., and Li, M. Why is spatial reasoning hard for vlms? an attention mechanism perspective on focus areas. *ICML*, 2025.

Cheng, A.-C., Yin, H., Fu, Y., Guo, Q., Yang, R., Kautz, J., Wang, X., and Liu, S. Spatialrgpt: Grounded spatial reasoning in vision language model. *NeurIPS*, 2024.

Cui, Y., Chen, H., Deng, H., Huang, X., Li, X., Liu, J., Liu, Y., Luo, Z., Wang, J., Wang, W., et al. Emu3. 5: Native multimodal models are world learners. *arXiv preprint arXiv:2510.26583*, 2025.

Deepmind, G. Veo3.1, 2025. URL <https://deepmind.google/models/veo/>.

Didolkar, A., Zadaianchuk, A., Awal, R., Seitzer, M., Gavves, E., and Agrawal, A. Ctrl-o: language-controllable object-centric visual representation learning. In *CVPR*, 2025.

Du, Y., Yang, S., Dai, B., Dai, H., Nachum, O., Tenenbaum, J., Schuurmans, D., and Abbeel, P. Learning universal policies via text-guided video generation. *NeurIPS*, 2023.

Foss, A., Evans, C., Mitts, S., Sinha, K., Rizvi, A., and Kao, J. T. Causalvqa: A physically grounded causal reasoning benchmark for video models. *arXiv preprint arXiv:2506.09943*, 2025.

Gao, S., Yang, J., Chen, L., Chitta, K., Qiu, Y., Geiger, A., Zhang, J., and Li, H. Vista: A generalizable driving world model with high fidelity and versatile controllability. *NeurIPS*, 2024. URL <https://arxiv.org/abs/2405.17398>.

Goyal, Y., Khot, T., Summers-Stay, D., Batra, D., and Parikh, D. Making the v in vqa matter: Elevating the role of image understanding in visual question answering. In *CVPR*, 2017.

Guo, J., Ye, Y., He, T., Wu, H., Jiang, Y., Pearce, T., and Bian, J. Mineworld: a real-time and open-source interactive world model on minecraft. *arXiv preprint arXiv:2504.08388*, 2025.

Ha, D. and Schmidhuber, J. World models. *arXiv preprint arXiv:1803.10122*, 2(3), 2018.

Hafner, D., Lillicrap, T., Norouzi, M., and Ba, J. Mastering atari with discrete world models. *ICLR*, 2021.

Hu, A., Russell, L., Yeo, H., Murez, Z., Fedoseev, G., Kendall, A., Shotton, J., and Corrado, G. Gaia-1: A generative world model for autonomous driving. *arXiv preprint arXiv:2309.17080*, 2023.

Hudson, D. A. and Manning, C. D. Gqa: A new dataset for real-world visual reasoning and compositional question answering. In *CVPR*, 2019a.

Hudson, D. A. and Manning, C. D. Gqa: A new dataset for real-world visual reasoning and compositional question answering. In *CVPR*, 2019b.

Johnson, J., Hariharan, B., Van Der Maaten, L., Fei-Fei, L., Lawrence Zitnick, C., and Girshick, R. Clevr: A diagnostic dataset for compositional language and elementary visual reasoning. In *CVPR*, 2017a.

Johnson, J., Hariharan, B., Van Der Maaten, L., Fei-Fei, L., Lawrence Zitnick, C., and Girshick, R. Clevr: A diagnostic dataset for compositional language and elementary visual reasoning. In *CVPR*, 2017b.

Johnson, J., Hariharan, B., Van Der Maaten, L., Fei-Fei, L., Lawrence Zitnick, C., and Girshick, R. Clevr: A diagnostic dataset for compositional language and elementary visual reasoning. In *CVPR*, 2017c.

Ko, P.-C., Mao, J., Du, Y., Sun, S.-H., and Tenenbaum, J. B. Learning to act from actionless videos through dense correspondences. *arXiv preprint arXiv:2310.08576*, 2023.

Koh, J. Y., Lee, H., Yang, Y., Baldridge, J., and Anderson, P. Pathdreamer: A world model for indoor navigation. In *ICCV*, 2021.

Langley, P. Crafting papers on machine learning. In *ICML*, 2000.

LeCun, Y. A path towards autonomous machine intelligence version 0.9. 2, 2022-06-27. *Open Review*, 62(1):1–62, 2022.

Li, B., Zhang, Y., Guo, D., Zhang, R., Li, F., Zhang, H., Zhang, K., Zhang, P., Li, Y., Liu, Z., et al. Llava-onevision: Easy visual task transfer. *arXiv preprint arXiv:2408.03326*, 2024.

Li, Y., Zhang, Y., Lin, T., Liu, X., Cai, W., Liu, Z., and Zhao, B. Sti-bench: Are mllms ready for precise spatial-temporal world understanding? *ICCV*, 2025.

Li, Z., Wang, X., Stengel-Eskin, E., Kortylewski, A., Ma, W., Van Durme, B., and Yuille, A. L. Super-clevr: A virtual benchmark to diagnose domain robustness in visual reasoning. In *CVPR*, 2023.

Lian, X., Yang, A., Zhu, J., Wang, P., and Zhang, Y. Imagine in space: Exploring the frontier of spatial intelligence and reasoning efficiency in vision language models. *arXiv preprint arXiv:2511.13782*, 2025.

Lin, J., Yu, Z., and Karlsson, B. F. Switch: Benchmarking modeling and handling of tangible interfaces in long-horizon embodied scenarios. *arXiv preprint arXiv:2511.17649*, 2025.

Ling, L., Lin, C.-H., Lin, T.-Y., Ding, Y., Zeng, Y., Sheng, Y., Ge, Y., Liu, M.-Y., Bera, A., and Li, Z. Scenethesis: A language and vision agentic framework for 3d scene generation. *arXiv preprint arXiv:2505.02836*, 2025.

Liu, F., Emerson, G., and Collier, N. Visual spatial reasoning. *ACL*, 2023.

Liu, Z., Gao, K., Liang, S., Xiao, B., Qiao, L., Ma, L., and Jiang, T. Beyond the visible: Benchmarking occlusion perception in multimodal large language models. *arXiv preprint arXiv:2508.04059*, 2025.

Locatello, F., Weissenborn, D., Unterthiner, T., Mahendran, A., Heigold, G., Uszkoreit, J., Dosovitskiy, A., and Kipf, T. Object-centric learning with slot attention. *NeurIPS*, 2020.

Long, X., Zhao, Q., Zhang, K., Zhang, Z., Wang, D., Liu, Y., Shu, Z., Lu, Y., Wang, S., Wei, X., et al. A survey: Learning embodied intelligence from physical simulators and world models. *arXiv preprint arXiv:2507.00917*, 2025.

Lu, T., Shu, T., Xiao, J., Ye, L., Wang, J., Peng, C., Wei, C., Khashabi, D., Chellappa, R., Yuille, A., et al. Genex: Generating an explorable world. *ICLR*, 2025.

Ma, W., Chen, H., Zhang, G., Chou, Y.-C., Chen, J., de Melo, C., and Yuille, A. 3dsrbench: A comprehensive 3d spatial reasoning benchmark. In *ICCV*, 2025.

OpenAI. Introducing gpt-5. <https://openai.com/index/introducing-gpt-5/>, 2025a.

OpenAI. Sora2 is here, 2025b. URL <https://openai.com/zh-Hans-CN/index/sora-2/>.

OpenAI. Why language models hallucinate, 2025c. URL <https://openai.com/index/why-language-models-hallucinate/>.

Parker-Holder, J., Ball, P., Bruce, J., Dasagi, V., Holsheimer, K., Kaplanis, C., Moufarek, A., Scully, G., Shar, J., Shi, J., et al. Genie 2: A large-scale foundation world model. URL: <https://deepmind.google/discover/blog/genie-2-a-large-scale-foundation-world-model>, 2024.

Parmar, P., Peh, E., and Fernando, B. Chainreaction! structured approach with causal chains as intermediate representations for improved and explainable causal video question answering. *arXiv preprint arXiv:2508.21010*, 2025.

Qi, Y., Zhao, H., Guo, Z., Ma, S., Chen, Z., Han, Y., Zhang, R., Lin, Z., Xin, S., Huang, Y., et al. Bear: Benchmarking and enhancing multimodal language models for atomic embodied capabilities. *arXiv preprint arXiv:2510.08759*, 2025.

Ray, A., Duan, J., Tan, R., Bashkirova, D., Hendrix, R., Ehsani, K., Kembhavi, A., Plummer, B. A., Krishna, R., Zeng, K.-H., et al. Sat: Spatial aptitude training for multimodal language models. *COLM*, 2024.

Seo, Y., Hafner, D., Liu, H., Liu, F., James, S., Lee, K., and Abbeel, P. Masked world models for visual control. In *CoRL*, pp. 1332–1344. PMLR, 2023.

Tang, Y., Qu, A., Wang, Z., Zhuang, D., Wu, Z., Ma, W., Wang, S., Zheng, Y., Zhao, Z., and Zhao, J. Sparkle: Mastering basic spatial capabilities in vision language models elicits generalization to spatial reasoning. *EMNLP*, 2024.

Team, G. G. Gemini 2.5 pro best for coding and highly complex tasks, 2025a. URL <https://deepmind.google/models/gemini/pro/>.

Team, G. G. Gemini2.5 flash: Best for fast performance on everyday tasks. <https://deepmind.google/models/gemini/flash/>, 2025b.

Team, Q. Qwen3-vl. <https://github.com/QwenLM/Qwen3-VL>, 2025c.

Tong, P., Brown, E., Wu, P., Woo, S., IYER, A. J. V., Akula, S. C., Yang, S., Yang, J., Middepogu, M., Wang, Z., et al. Cambrian-1: A fully open, vision-centric exploration of multimodal llms. *NeurIPS*, 2024a.

Tong, S., Brown, E., Wu, P., Woo, S., Middepogu, M., Akula, S. C., Yang, J., Yang, S., Iyer, A., Pan, X., et al. Cambrian-1: A fully open, vision-centric exploration of multimodal llms. *NIPS*, 2024b.

Wan, T., Wang, A., Ai, B., Wen, B., Mao, C., Xie, C.-W., Chen, D., Yu, F., Zhao, H., Yang, J., et al. Wan: Open and advanced large-scale video generative models. *arXiv preprint arXiv:2503.20314*, 2025.

Wang, A., Huang, H., Fang, J. Z., Yang, Y., and Ma, C. Ati: Any trajectory instruction for controllable video generation. *arXiv preprint arXiv:2505.22944*, 2025a.

Wang, J., Ye, L., Lu, T., Xiao, J., Zhang, J., Guo, Y., Liu, X., Chellappa, R., Peng, C., Yuille, A., et al. Evoworld: Evolving panoramic world generation with explicit 3d memory. *arXiv preprint arXiv:2510.01183*, 2025b.

Wang, X., Ma, W., Zhang, T., de Melo, C. M., Chen, J., and Yuille, A. Spatial457: A diagnostic benchmark for 6d spatial reasoning of large multimodal models. In *CVPR*, 2025c.

Wu, D., Liu, F., Hung, Y.-H., and Duan, Y. Spatial-mllm: Boosting mllm capabilities in visual-based spatial intelligence. *NeurIPS*, 2025a.

Wu, H., Huang, X., Chen, Y., Zhang, Y., Wang, Y., and Xie, W. Spatialscore: Towards unified evaluation for multimodal spatial understanding. *arXiv preprint arXiv:2505.17012*, 2025b.

Wu, P., Escontrela, A., Hafner, D., Abbeel, P., and Goldberg, K. Daydreamer: World models for physical robot learning. In *CoRL*, pp. 2226–2240. PMLR, 2023a.

Wu, Z., Dvornik, N., Greff, K., Kipf, T., and Garg, A. Slotformer: Unsupervised visual dynamics simulation with object-centric models. *ICLR*, 2023b.

Yang, M., Du, Y., Ghasemipour, K., Tompson, J., Schurmans, D., and Abbeel, P. Learning interactive real-world simulators. *arXiv preprint arXiv:2310.06114*, 1(2): 6, 2023.

Yang, S., Yang, J., Huang, P., Brown, E., Yang, Z., Yu, Y., Tong, S., Zheng, Z., Xu, Y., Wang, M., et al. Cambrian-s: Towards spatial supersensing in video. *arXiv preprint arXiv:2511.04670*, 2025.

Yu, H.-X., Duan, H., Herrmann, C., Freeman, W. T., and Wu, J. Wonderworld: Interactive 3d scene generation from a single image. *CVPR*, 2025a.

Yu, J., Qin, Y., Wang, X., Wan, P., Zhang, D., and Liu, X. Gamefactory: Creating new games with generative interactive videos. *arXiv preprint arXiv:2501.08325*, 2025b.

Zhang, H., Wang, Z., Lyu, Q., Zhang, Z., Chen, S., Shu, T., Dariush, B., Lee, K., Du, Y., and Gan, C. Combo: compositional world models for embodied multi-agent cooperation. *arXiv preprint arXiv:2404.10775*, 2024.

Zhen, H., Qiu, X., Chen, P., Yang, J., Yan, X., Du, Y., Hong, Y., and Gan, C. 3d-vla: A 3d vision-language-action generative world model. *ArXiv*, abs/2403.09631, 2024. URL <https://api.semanticscholar.org/CorpusID:268385444>.

Zhen, H., Sun, Q., Zhang, H., Li, J., Zhou, S., Du, Y., and Gan, C. Tesseract: learning 4d embodied world models. *arXiv preprint arXiv:2504.20995*, 2025.

Zhou, F., Huang, J., Li, J., Ramanan, D., and Shi, H. Pai-bench: A comprehensive benchmark for physical ai. *arXiv preprint arXiv:2512.01989*, 2025a.

Zhou, S., Du, Y., Chen, J., Li, Y., Yeung, D. Y., and Gan, C. Robodreamer: Learning compositional world models for robot imagination. *ArXiv*, abs/2404.12377, 2024. URL <https://api.semanticscholar.org/CorpusID:269214356>.

Zhou, S., Vilesov, A., He, X., Wan, Z., Zhang, S., Nagachandra, A., Chang, D., Chen, D., Wang, X. E., and Kadambi, A. Vlm4d: Towards spatiotemporal awareness in vision language models. In *ICCV*, 2025b.

## A. Outline of Appendix

The Appendix is organized as follows:

- **Section C** presents the details of our data collection and annotation process. We provide examples of each question template and examples of {Image, Question, Answer} triplets of each reasoning type in this section.
- **Section D** presents the details of the evaluation protocol.
- **Section E** presents additional results analysis. We present a full comparison with standard deviations and reasoning analysis in this section.
- **Section F** presents the additional details of COW.
- **Section G** presents the additional experiment results and analysis of COW. We present visualization, failure case analysis, and additional discussion in this section.
- **Section H** presents the examples from each category in our benchmark.

## B. Benchmark Comparison

Benchmark	Evaluation				Design	
	2D	3D	TD	CP	OM	RL
CLEVR-Count (Johnson et al., 2017b)	✓					
CLEVR (Johnson et al., 2017a)	✓				✓	
VQA (Goyal et al., 2017)	✓				✓	
GQA (Hudson & Manning, 2019a)	✓				✓	
CV-Bench (Tong et al., 2024a)	✓	✓			✓	
SAT (Ray et al., 2024)	✓	✓	✓		✓	
STI-Bench (Li et al., 2025)	✓	✓	✓		✓	
Spatial457 (L1-L4) (Wang et al., 2025c)	✓	✓		✓		
CausalVQA (Foss et al., 2025)	✓		✓	✓	✓	
VSI-Super (Yang et al., 2025)	✓	✓	✓		✓	
<b>CausalSpatial</b>	✓	✓	✓	✓	✓	✓

**Table 3. Comparison of benchmarks.** **2D** denotes 2D perception; **3D** denotes 3D static relation; **TD** denotes Temporal Dynamics; **CP** denotes Causal Prediction. **OM** denotes Object-level Manipulation. **RL** denotes Realistic. CausalSpatial involves diverse paradigms of spatial reasoning, spanning from 2D perception to temporal dynamics. CausalSpatial incorporates causal prediction into spatial reasoning, paving the way for the next generation of vision intelligence.

The items in **Evaluation** columns are associated with Figure 1, including three different levels of spatial reasoning. **2D perception** is the fundamental capability of spatial reasoning, followed by **3D static relation** on which most of existing spatial reasoning benchmarks focus. **Temporal dynamics** takes a step further towards causal spatial reasoning. It requires models to reason about the dynamic process anchored to the question image. **Causal prediction** restricts models’ reasoning to follow the real-world physics laws and other constraints.

The items in **Design** columns concentrate on the characteristics and quality of benchmarks. **Object manipulation** is consistent with our object-centric design nature. The questions in CausalSpatial imply specific object-level motion interventions. **Realistic** emphasizes the quality of images in benchmarks. The scenarios in CausalSpatial are rendered with high-quality and realistic assets.

## C. Benchmark Data Collection

To comprehensively evaluate the causal spatial reasoning capabilities of MLLMs, CausalSpatial is constructed upon fully annotated 3D scene structures that include RGB images, depth maps, and oriented bounding boxes for each object. For every

scene, multiple questions are generated with distinct action prompts that specify hypothetical or counterfactual motions. The resulting events are then physically simulated and rendered using physical engines, ensuring that all outcomes are consistent with real-world dynamics and physically plausible interactions.

### C.1. Objects

We collect a diverse set of publicly available 3D object assets spanning multiple semantic categories, including vehicles, decorative items, indoor utilities, sports items (basketball, soccer, and billiards) and everyday objects such as furniture, different containers, and fruits, with more than 50 object types. To enhance visual realism and diversity, we manually refine the textures and curate a consistent color palette for each object. All assets are standardized in scale, material properties, and orientation to ensure coherence across scenes and to enable stable, physically accurate simulations within the rendering environment. This diversity enables CausalSpatial to cover a broad range of spatial interactions, supporting comprehensive evaluation of object-level causal reasoning.

### C.2. Background

To ensure visual realism and physical plausibility, all images in CausalSpatial are rendered from fully configured 3D environments. Each scene is composed with carefully arranged backgrounds and lighting conditions to preserve depth cues and contextual coherence. Overall, we sample over 130 diverse camera viewpoints across different elevations and azimuths, capturing rich spatial variability while maintaining consistent scene geometry. This design enables models to perceive spatial layouts from multiple perspectives, supporting robust evaluation of viewpoint-invariant causal reasoning.

For each reasoning type introduced in Sec. 2.2, we design a set of motion prompts  $M_0, \dots, M_k$  with explicit directional cues that define object movements. To minimize ambiguity in textual descriptions, motion representations are expressed either as clear textual instructions (for objects with well-defined orientations) or as trajectory arrows (for symmetric objects). GPT-5 is employed to generate and refine object description prototypes for precise object identification, which are subsequently reviewed by human annotators to ensure linguistic clarity and eliminate ambiguity among visually similar objects. A comprehensive set of question templates (as listed in Figure 12, Figure 13, and Figure 14) used for benchmark construction is provided in the Appendix. For consistency and ease of evaluation, all questions are formatted as multiple-choice queries with an additional “not sure” option included to mitigate random guessing and short-cut biases.

### C.3. Dynamics rendering for answer generation

After configuring each static scene, we record the center coordinates ( $x, y, z$ ) and orientation angles (pitch, roll, yaw) for every object in the scene. After sampling a motion  $M_i$ , to ensure accurate supervision and physical realism, we simulate each object motion by assigning a constant initial velocity vector  $(v_x, v_y, v_z)$  and executing the dynamics within Blender’s Bullet Physics Engine. The simulated scenes are rendered as photo-realistic image sequences that capture realistic trajectories and physically consistent interactions. During this process, the mesh intersection situation is calculated to generate ground truth answer for each question. The first frame of each image sequence is then paired with its corresponding causal reasoning QA to form the final evaluation samples in CausalSpatial.

## D. Additional Evaluation Details

During evaluation, all images are uniformly resized to a resolution of  $1920 \times 1080$  (width  $\times$  height) to preserve the global scene layout and ensure that fine-grained spatial cues (*e.g.*, object boundaries, depth ordering, contact geometry, and subtle occlusion relationships) remain clearly distinguishable to the model. Each benchmark instance is formatted as a multiple-choice question with four candidate answers and an additional “Not Sure” option, which is included to discourage forced predictions and provide a clearer measurement of model uncertainty under ambiguous or visually challenging conditions.

To prevent positional bias and mitigate shortcut exploitation, the ordering of answer choices is independently randomized for every sample. All models are evaluated in a single-turn inference setting with explicit reasoning chain-of-thought prompting.

Model	Level 1					Level 2					Avg.
	Col.	Com.	Occ.	Traj.	Avg.	Col.	Com.	Occ.	Traj.	Avg.	
<b>Spatial Reasoning MLLMs</b>											
Spatial-VLM(Chen et al., 2024)	20.98 $\pm$ 1.01	47.62 $\pm$ 5.72	48.15 $\pm$ 6.11	46.88 $\pm$ 2.97	36.24 $\pm$ 1.59	15.75 $\pm$ 1.92	41.67 $\pm$ 1.96	24.07 $\pm$ 1.85	37.96 $\pm$ 2.58	28.25 $\pm$ 1.48	33.50 $\pm$ 1.26
Spatial-MLLM(Wu et al., 2025a)	41.96 $\pm$ 1.09	55.56 $\pm$ 0.00	48.15 $\pm$ 0.74	54.17 $\pm$ 1.56	47.93 $\pm$ 0.21	24.41 $\pm$ 1.92	44.44 $\pm$ 4.39	12.96 $\pm$ 0.00	24.82 $\pm$ 1.46	24.56 $\pm$ 0.57	40.00 $\pm$ 0.07
<b>Open-source MLLMs</b>											
LLaVAOneVision1.5-8B-I. (Li et al., 2024)	43.01 $\pm$ 0.77	42.86 $\pm$ 8.09	38.52 $\pm$ 1.05	29.17 $\pm$ 2.68	38.17 $\pm$ 0.38	15.38 $\pm$ 3.04	41.67 $\pm$ 4.39	20.37 $\pm$ 4.72	38.69 $\pm$ 1.46	27.84 $\pm$ 1.27	34.62 $\pm$ 0.63
Qwen2.5-VL-7B-I.(Team, 2025c)	41.75 $\pm$ 2.10	42.86 $\pm$ 2.51	42.22 $\pm$ 2.62	44.27 $\pm$ 1.84	42.66 $\pm$ 1.16	30.40 $\pm$ 6.80	41.67 $\pm$ 12.58	24.07 $\pm$ 4.14	38.69 $\pm$ 9.74	33.79 $\pm$ 4.67	39.61 $\pm$ 1.18
Qwen3-VL-2B-I.(Team, 2025c)	47.43 $\pm$ 1.97	47.62 $\pm$ 5.61	49.63 $\pm$ 3.99	43.23 $\pm$ 1.04	46.69 $\pm$ 1.04	19.35 $\pm$ 6.93	38.89 $\pm$ 11.95	22.22 $\pm$ 9.44	37.96 $\pm$ 5.11	28.98 $\pm$ 3.56	40.60 $\pm$ 1.62
Qwen3-VL-4B-I.(Team, 2025c)	47.55 $\pm$ 1.78	50.79 $\pm$ 8.09	48.15 $\pm$ 2.96	44.79 $\pm$ 2.60	47.19 $\pm$ 1.25	24.41 $\pm$ 6.80	44.44 $\pm$ 3.93	16.67 $\pm$ 5.86	62.77 $\pm$ 1.46	40.11 $\pm$ 1.27	44.76 $\pm$ 1.19
Qwen3-VL-8B-I.(Team, 2025c)	41.40 $\pm$ 0.55	66.67 $\pm$ 13.70	51.11 $\pm$ 2.22	47.92 $\pm$ 0.82	47.55 $\pm$ 0.96	22.76 $\pm$ 3.04	36.11 $\pm$ 2.78	29.63 $\pm$ 3.70	50.36 $\pm$ 4.44	35.85 $\pm$ 2.79	43.53 $\pm$ 0.53
Qwen3-VL-8B-T.(Team, 2025c)	42.74 $\pm$ 1.43	63.49 $\pm$ 5.02	48.15 $\pm$ 2.67	55.73 $\pm$ 1.84	49.43 $\pm$ 0.23	23.75 $\pm$ 3.04	44.44 $\pm$ 8.10	22.22 $\pm$ 1.85	34.31 $\pm$ 0.52	29.71 $\pm$ 0.91	42.65 $\pm$ 0.15
Qwen3-VL-30B-A3B-I.(Team, 2025c)	47.02 $\pm$ 1.57	55.56 $\pm$ 3.55	48.15 $\pm$ 2.62	47.40 $\pm$ 3.33	48.15 $\pm$ 0.53	30.16 $\pm$ 7.32	52.78 $\pm$ 11.45	31.48 $\pm$ 6.68	52.55 $\pm$ 3.26	41.32 $\pm$ 1.04	45.80 $\pm$ 0.66
Qwen3-VL-30B-A3B-T.(Team, 2025c)	52.99 $\pm$ 1.43	58.73 $\pm$ 4.05	51.11 $\pm$ 2.22	54.17 $\pm$ 3.49	53.49 $\pm$ 1.13	35.09 $\pm$ 1.36	63.89 $\pm$ 12.42	46.30 $\pm$ 7.97	48.18 $\pm$ 2.13	44.79 $\pm$ 3.52	50.50 $\pm$ 1.82
<b>Closed-source MLLMs</b>											
GPT5(OpenAI, 2025a)	49.65 $\pm$ 2.08	61.90 $\pm$ 6.35	59.26 $\pm$ 1.48	54.17 $\pm$ 5.21	54.00 $\pm$ 3.24	40.94 $\pm$ 0.00	50.00 $\pm$ 0.00	62.96 $\pm$ 1.85	64.96 $\pm$ 1.46	54.52 $\pm$ 0.36	54.17 $\pm$ 2.40
GPT5-mini(OpenAI, 2025a)	37.76 $\pm$ 2.08	42.86 $\pm$ 2.38	48.15 $\pm$ 8.15	44.79 $\pm$ 1.04	42.31 $\pm$ 2.83	35.43 $\pm$ 3.85	47.22 $\pm$ 2.78	50.00 $\pm$ 3.70	67.88 $\pm$ 2.19	51.41 $\pm$ 0.64	45.44 $\pm$ 2.28
Gemini2.5 Pro(Team, 2025a)	43.62 $\pm$ 3.46	63.49 $\pm$ 3.17	60.00 $\pm$ 5.19	53.12 $\pm$ 2.08	51.44 $\pm$ 3.39	30.65 $\pm$ 1.92	52.78 $\pm$ 2.78	48.15 $\pm$ 14.81	64.96 $\pm$ 0.73	48.85 $\pm$ 3.94	50.55 $\pm$ 1.25
Gemini2.5 Flash(Team, 2025b)	46.21 $\pm$ 0.98	50.79 $\pm$ 11.51	48.89 $\pm$ 4.10	56.25 $\pm$ 2.89	50.02 $\pm$ 2.42	42.31 $\pm$ 10.04	58.33 $\pm$ 2.95	25.93 $\pm$ 7.00	55.47 $\pm$ 1.83	46.53 $\pm$ 1.71	48.82 $\pm$ 1.75
Sonnet 3.7(Anthropic, 2025)	55.00 $\pm$ 1.04	49.21 $\pm$ 1.59	45.56 $\pm$ 6.30	46.35 $\pm$ 0.00	50.12 $\pm$ 1.84	29.41 $\pm$ 0.00	48.61 $\pm$ 1.39	34.26 $\pm$ 0.93	60.58 $\pm$ 0.73	44.16 $\pm$ 0.36	48.07 $\pm$ 1.41
Human	86.84	80.00	92.50	82.50	85.44	78.57	97.22	97.50	62.50	83.54	84.49
Random	23.61	31.75	32.35	38.54	30.34	8.54	33.33	20.37	32.14	24.50	28.6

Table 4. The performance of MLLMs on CausalSpatial. Col. denotes Collision. Com. denotes Compatibility. Occ. denotes Occlusion.

Traj. denotes Trajectory. Avg. denotes Average scores. Best &amp; Second best.

## E. Additional Results

In this section, we provide an extended analysis of model behavior beyond the main paper results. We examine not only the quantitative differences among various MLLMs, but also the underlying factors that drive these performance gaps across tasks. Together, these results offer a deeper understanding of the capabilities and limitations of current multimodal models in spatial and causal reasoning.

### E.1. Comparison Results

In Table 4, we present the performance of various MLLMs across diverse causal spatial tasks and difficulties on CausalSpatial. We compare proprietary models (e.g., GPT-5, Gemini 2.5 Pro), open-source general models (e.g., Qwen3-VL series, LLaVAOneVision), and open-source spatial intelligence models (e.g., Spatial-VLM, Spatial-MLLM) to assess their causal spatial reasoning capabilities.

**Comparison across diverse model groups.** The results reveal distinct performance tiers among the evaluated groups. Closed-source frontier models generally lead the benchmark, with GPT-5 achieving a strong average score of 54.17%, followed closely by Gemini 2.5 Pro at 50.55%. Top-tier open-source models have largely closed the gap, with the best-performing Qwen3-VL-30B-A3B-Thinking reaching 50.50%, surpassing all proprietary counterparts. Conversely, spatially-tuned models struggle, with Spatial-VLM and Spatial-MLLM averaging only 33.50% and 40.00%. This indicates that current spatial tuning prioritizes static perception over the causal spatial reasoning demanded by our benchmark. Furthermore, despite the advancements in general MLLMs, a substantial gap remains between the best model performance (~55%) and human performance (84.49%), highlighting the challenging nature of causal spatial reasoning.

**Comparison in Qwen series.** The Qwen3-VL series serves as an excellent testbed for analyzing the effects of model scaling and reasoning mechanisms. As shown in Table 4, the performance does not follow a strict linear scaling law. While the comprehensive score improves from 2B (40.60%) to 4B (44.76%), it exhibits a slight decline for the 8B model (43.53%), reaching a performance plateau. Additionally, extra “thinking” mode training fails to lead to consistent performance improvement. For the 8B model, enabling the thinking mode results in a performance regression (dropping from 43.53% to 42.65%), whereas for the 30B model, the thinking mechanism unlocks significant potential, boosting performance from 45.80% to 50.50%. This contrast indicates that while larger models can effectively leverage extended reasoning for causal spatial tasks, smaller models may struggle to utilize the additional tokens effectively, potentially leading to reasoning errors.

**Comparison in Proprietary Models.** We further examine frontier models to understand the trade-offs between capability balance and model capacity. As detailed in Table 4, GPT-5 achieves the leading position among proprietary models with an average score of 54.17%, demonstrating robust performance across diverse spatial tasks. Gemini 2.5 Pro follows with a competitive score of 50.55%, while Claude 3.7 Sonnet records 48.07%. Notably, we observe a sharp performance decline when transitioning to lightweight model variants. For instance, GPT-5 outperforms its mini counterpart by nearly 9 percentage points (54.17% vs. 45.44%). This consistent gap confirms that causal spatial reasoning is a capacity-hungry task,

where lightweight models lack the sufficient depth to simulate complex physical interactions.

To examine why performance shows limited gain despite significantly longer generation from reasoning-oriented models, we analyze the reasoning traces produced on causal spatial tasks. Upon our analysis, MLLMs reliably recognize static layouts and object placements. However, in failure cases, the visual information in the image is either weakly integrated or incorrectly interpreted. When this happens, the model’s reasoning becomes dominated by generic linguistic patterns learned during instruction tuning, rather than by the specific spatial geometry present in the scene. For example, in the car–cabinet scenario, the model generates a long and seemingly coherent explanation but overlooks the salient visual fact that the car is directly in front of the wooden calendar. Likewise, in the banana–box example, the model infers that the banana exceeds the box depth, which an assumption not supported by the actual image. These cases demonstrate that additional language tokens do not lead to better causal reasoning; the model’s chain-of-thought becomes verbose but not more visually grounded. Consequently, the model reaches incorrect causal conclusions even when its textual reasoning appears logically structured.

### E.1.1. FINDINGS

While MLLMs have shown proficiency in static perception, our results indicate a fundamental struggle in transitioning to dynamic causal reasoning. In this section, we analyze the limitations of current model evolution paths. We find that the prevailing approaches, such as scaling up parameters and employing extended textual reasoning, yield diminishing returns on CausalSpatial. This suggests that the challenge cannot be solved merely by “more compute” or “more tokens”, but requires a fundamental shift in how models ground their reasoning in physical reality.

**Finding 1:** *Improvement in causal spatial reasoning capability requires more than model scaling or spatial-centric fine-tuning.*

Crucially, as detailed in Figure 3, we observe diminishing returns from model scaling within the Qwen3-VL series. The instruction-tuned variants exhibit performance plateaus, with the 4B, 8B, and 30B-A3B models achieving similar scores of 44.76%, 43.53%, and 45.80%, respectively. This saturation emphasizes that simply scaling up parameters is insufficient to master causal spatial reasoning.

Regarding data strategy, domain-specific spatial training provides no clear advantage. Surprisingly, the Qwen3-VL-8B-T, despite its enhanced spatial training, fails to exhibit surpass the base instruction version (43.53% for the Instruction version and 42.65% for the Thinking version). Similarly, specialized spatial reasoning MLLMs (e.g., Spatial-VLM and Spatial-MLLM) significantly underperform general-purpose MLLMs (e.g., Qwen2.5-VL-7B-I and Qwen3-VL series). These results suggest that existing spatial tuning (optimized for “where is something”) struggles to address “what will happen”, underscoring the necessity of moving toward temporally consistent reasoning frameworks for causality reasoning.

**Finding 2:** *Extended textual reasoning inflates model confidence without yielding proportional accuracy gains.*

We observe a decoupling between model confidence and accuracy performance. Larger models become increasingly decisive, often unwarranted. As shown in Figure 3, scaling model parameters dramatically reduces uncertainty. The Not Sure Rate (NSR) falls from 18.77% on Qwen3-VL-4B-I to nearly zero (0.10%) on Qwen3-VL-30B-A3B-T. This trend is further exacerbated by the thinking mode, where the NSR drops even more aggressively (e.g., from 10.57% (I) to 2.37% (T) on Qwen3-VL-8B, from 2.84% (I) to 0.10% (T) on Qwen3-VL-30B-A3B). However, this decisiveness is deceptive. The sharp decrease in uncertainty is not accompanied by a corresponding leap in accuracy.

## F. Implementation Details of COW

**CAUSAL OBJECT WORLD MODEL** (COW) is a modular world model framework. It can be adopted in the causal spatial reasoning scenarios, such as occlusion, compatibility, collision, and Trajectory. COW consists of four primary steps: instance grounding, motion analysis, trajectory computation, and video generation.

### F.1. Instance Grounding

Each question in CausalSpatial consists of an image depicting the current spatial state and a question text that implies a specific motion. At the core of causal spatial reasoning lies the notion of an instance: the entity whose spatial state first undergoes change and subsequently interacts with other entities. Accordingly, the initial stage of our COW focuses on instance grounding.

To identify the instance involved in the motion, we employ an MLLM (Qwen3-VL-A3B) to interpret the instance that involves the motion described in the question. For simple cases, for example, the query “the car is moving forward”, the model can readily determine that “the car” is the instance whose state changes. More complex scenarios require finer-grained grounding. For example, in the scenario of billiards collisions, the image may contain multiple billiards balls, and the moving ball must be explicitly distinguished (*e.g.*, “the red number-5 ball”, “the white ball”, “the black ball”). To handle this, we first prompt the MLLM to generate a precise textual description of the moving instance. Then, given this description, we further prompt the model to localize the pixel coordinate  $(x_p, y_p)$  of the corresponding instance within the image.

## F.2. Motion Analysis

The second step in our pipeline is to analyze the motion described in the question. Our questions typically involve two distinct categories of moving instances, each requiring a different approach for motion analysis. The first category includes instance with a clearly defined orientation, such as “the car”. In these cases, the query might describe the motion in terms of specific directions, like “moving forward” or “moving to the left”. To determine the exact direction of motion, we rely on the relative positioning of the instance orientation within the image. We can infer the concrete direction of movement by analyzing these positional relationships.

The second category involves instances that lack clear orientation, such as billiards balls, vases, or basketballs. For these instances, the image includes explicit visual cues, such as arrows, to indicate the direction of motion. Additionally, the motion direction is parallel to the arrow’s direction, but the query itself determines whether the arrow should be considered positive or negative. We prompt the MLLM to identify the direction of the arrow in the image, and based on the question’s context, we assign the appropriate positive or negative value to the motion direction.

## F.3. Trajectory Computation

After obtaining both the pixel coordinates of the target instance and its motion direction, we proceed to simulate its movement. We first preset the number of frames and assign a constant velocity. The position of the instance is defined as the center pixel coordinate of its bounding box in the initial frame. By combining the motion direction with the preset velocity and frame count, we compute a sequence of center coordinates that represent the instance’s movement over time. This produces a series of pixel-level positions, forming the trajectory tensors of the moving instance.

## F.4. Video Generation

After the trajectory tensors are obtained, we feed the detailed motion description, the question image, and the constructed trajectory tensors into the ATI video generation model to synthesize the simulation video. The question image provides the initial spatial state of the scene. The motion description supplies additional semantic cues for generating motion-consistent content. The trajectory tensor explicitly controls the instance’s movement.

Concretely, the input image is first encoded by a VAE encoder into a latent feature map  $L_1 \in R^{H \times W \times C}$ . For the input trajectory, ATI uses the starting location of the point in the first frame to bilinearly sample a  $C$ -dimensional feature vector from  $L_1$ , which serves as the appearance feature associated with that trajectory.

Furthermore, we randomly sample a few static points which is away from the motion trajectory, used for fixing the camera view. Therefore, for each generation, we have a trajectory tensor  $\phi_M = (x_t, y_t)_{t=0}^T$  and a set of static points  $\Phi_s = \{\phi_s\}^N$ , where  $\{\phi_s = (x_i, y_i)_{t=0}^T\}$ . In total, the input trajectory is  $\Phi = \{\phi_M, \Phi_s\}$ . ATI then constructs, at each frame  $t$ , a spatial Gaussian mask centered at  $(x_t, y_t)$  in the latent grid. This mask softly spreads the sampled feature to nearby latent pixels, assigning larger weights to positions closer to the trajectory point and decaying smoothly with distance. In this way, the same appearance feature is propagated along the trajectory over time.

These trajectory-conditioned latent features are then injected into the pre-trained image-to-video DiT backbone as an additional conditioning signal. During denoising, the DiT blocks jointly process the noisy video latents and the injected trajectory features, guiding the diffusion process to follow the specified motion paths while preserving semantic and visual coherence. Finally, the denoised video latents are decoded by the VAE decoder into RGB frames, producing a video whose motion is aligned with the user-provided trajectories. In practice, ATI can be plugged into different I2V backbones (Wan2.1-14B) without retraining them from scratch, and simple regularization strategies such as tail-dropout are applied during training to avoid artifacts when trajectories terminate early.

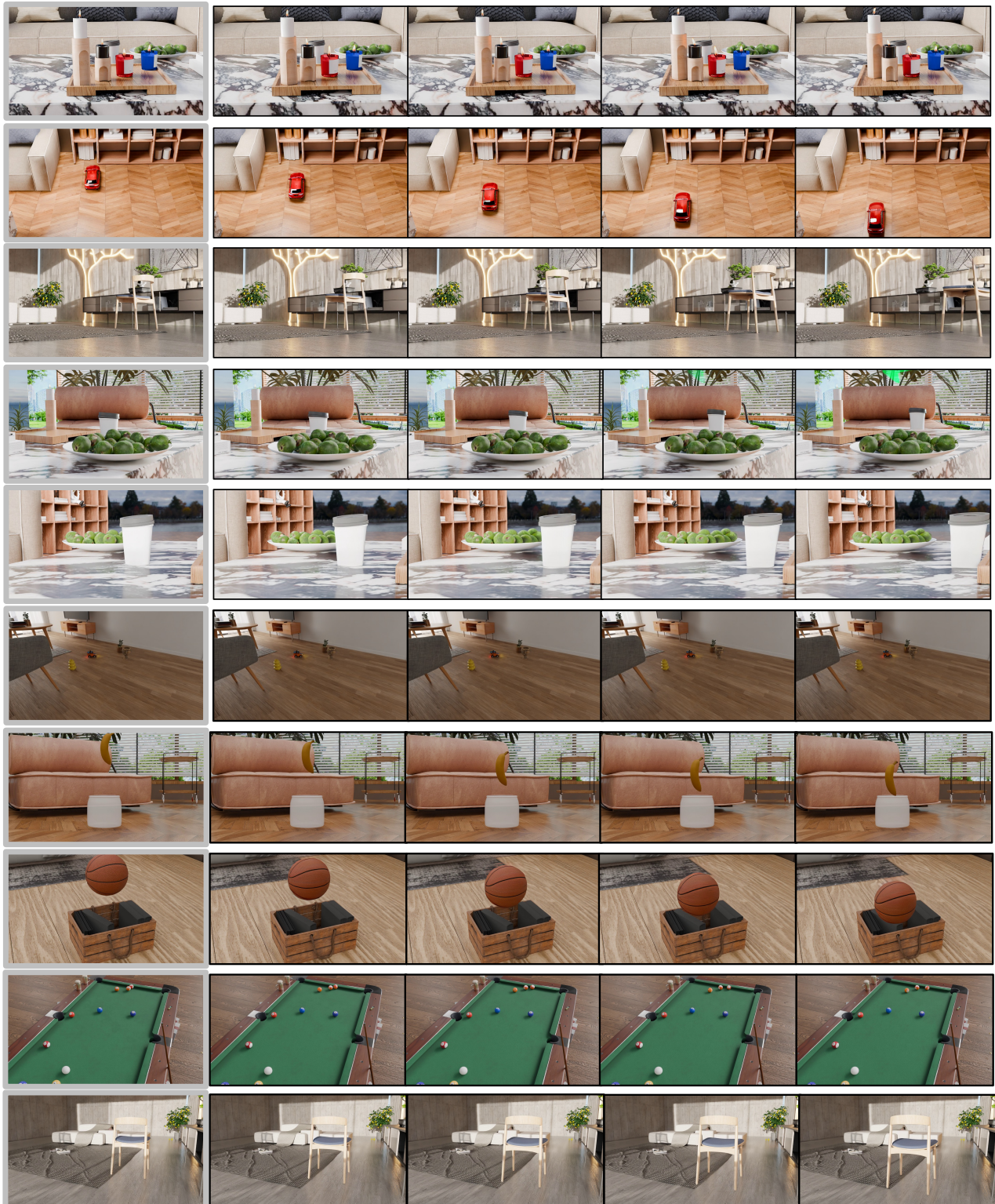


Figure 7. Additional visualizations of COW across diverse indoor and outdoor scenes. Despite the presence of noisy backgrounds with complex object arrangements, COW consistently preserves object boundaries and appearance, maintains stable geometric reasoning, and produces coherent spatial predictions. This explicit visual information helps MLLMs with causal spatial reasoning tasks.

## G. Additional Analysis of COW

To further understand the behavior and limitations of our framework, we conduct an extended analysis of COW beyond the main experiments. This section provides a deeper examination of how the model behaves under diverse spatial configurations, including both successful and problematic scenarios. We first present qualitative visualizations, and then analyze failure cases in Collision and Trajectory cases.

### G.1. Visualization

We provide additional qualitative results in this section to further illustrate the behavior of COW across a variety of settings. As shown in the examples in Figure 7, COW generates plausible and coherent video rollouts that faithfully reflect the parsed trajectories. Even in visually cluttered or geometrically complex scenes, the method demonstrates strong instance-level controllability, accurately preserving object identity, motion direction, and interaction patterns throughout the simulated sequence. Moreover, the generated rollouts exhibit high physical plausibility, as shown in the billiards example: different balls move along feasible paths, maintain realistic collision dynamics, and satisfy basic physical constraints of collision responses.

These improvements underscore the central role of grounded visual evidence during test-time reasoning. When models are provided with short simulated rollouts that explicitly encode object geometry, spatial layout, and anticipated interactions, their reasoning becomes more consistent and less reliant on implicit world assumptions. The results also demonstrate that richer visual context strengthens the benefits of test-time scaling strategies, enabling models to reason more reliably under ambiguity.

### G.2. Failure Cases of COW

We observe that the primary challenge often stems from the ambiguity of estimating physical parameters from a single static image. Inaccuracies in parsing initial states, such as misinterpreting the gravitational vertical or object orientation, can propagate downstream, resulting in simulated trajectories that deviate from the true causal spatial reasoning (*e.g.*, objects appearing to “fall” sideways due to incorrect gravity vectors). At the same time, collision, which includes complex object dynamics, remains a hard question for the community. We find that these problems limit the performance improvements of COW in Collision and Trajectory categories. However, despite the potential noise introduced by this error accumulation, our COW framework demonstrates robustness to a certain extent, and it delivers a consistent average improvement in performance.

## H. Data Examples

To illustrate the diversity and structure of our benchmark, we provide representative examples from each of the four core causal spatial reasoning tasks: collision (in Figure 8), compatibility (in Figure 9), occlusion (in Figure 11), and physics-based interaction (in Figure 10). Each example contains (i) the rendered scene, (ii) the queried causal spatial question, and (iii) the corresponding ground-truth outcome used for evaluation. Examples from both **Level1 (one-to-one)** and **Level2 (one-to-multiple)** are provided. Together, these examples demonstrate the range of object arrangements, geometric configurations, and causal dependencies present in CausalSpatial.

### H.1. Question generation

## Collision



Level1:

There is a toy car in the picture among several nearby objects. Please focus only on the objects on the floor and ignore all furniture, including the chair, bed, table, shelf, and cabinet. From the car's perspective, answer the following question:  
A toy pickup truck with a light-colored body lies on the floor. Could it bump into something if it proceeds forward?

Answer by (A) Yes, (B) No or (C) Not sure.

**GT: (A) Yes**

Level2:

There is a toy car in the picture among several nearby objects. Please focus only on the objects on the floor and ignore all furniture, including the chair, bed, table, shelf, and cabinet. From the car's perspective, answer the following question:  
You can see an orange toy vehicle on the floor. If it starts to move forward, is it enough to remove the vase with green plants to prevent all collisions? If removing the vase with green plants is insufficient, what else should be done to avoid collisions?

- (A) Remove the soft, pale grayish-white vase with moon pattern;
- (B) There is no collision;
- (C) Remove UFO-shaped yellow vase;
- (D) Removing the vase with green plants is sufficient;
- (E) Not sure;
- (F) Remove the white vase with a twisted loop.

If you determine there is no collision, please select the option indicating no collision.

Answer by (A) Yes, (B) No or (C) Not sure.

**GT: (C) Remove UFO-shaped yellow vase**

Figure 8. Examples of counterfactual collision reasoning in CausalSpatial.

## Compatibility



Level1:

If the banana falls freely from its current position, can it fit into the wooden box? 'Fit into' means it doesn't exceed the horizontal plane of the wooden box's opening.

Answer by (A) Yes, (B) No or (C) Not sure.

**GT: (A) Yes**



Level2:

Now there are already some books in the wooden box. If the apple falls freely from its current position, can it fit into the wooden box? 'Fit into' means it doesn't exceed the horizontal plane of the wooden box's opening.

Answer by (A) Yes, (B) No or (C) Not sure.

**GT: (A) Yes**

Figure 9. Examples of hypothetical compatibility reasoning in CausalSpatial.

## Physics



Level1:

Based on the soccer ball's trajectory shown in the image (Note: The red box indicates the starting point of the trajectory), will the ball go into the goal?

Answer by (A) Not sure; (B) Yes; (C) No.

**GT: (C) No**



Level2:

If the billiard ball moves in the direction of the red arrow, will any ball go into the pocket and score? Note: Only consider direct shots and ball-to-ball collisions. Ignore the table cushion bounces.

Answer by (A) Yes, (B) No or (C) Not sure.

**GT: (B) No**

Figure 10. Examples of physics-grounded spatial anticipation task in CausalSpatial.

## Occlusion



### Level 1:

Now I want to move the chair to make the potted orange tree visible. If the chair moves backward by the distance of one chair, would the potted orange tree be revealed or occluded?

**Note:** All directions (left, right, forward, backward) are relative to the chair's own coordinate system, and the chair moves straight along the direction by the length of one chair.

Answer by (A) Revealed, (B) Occluded or (C) Not sure.

**GT: (A) Revealed**



### Level2:

Given the scene where the red and blue arrows denote two perpendicular edges of the desk, and the tray contains four candles (blue, red, white, and black), consider the following planning task: You are asked to predict how the occlusion relationship between two objects will evolve over a planned motion.

The white candle will move *along the edge of the tray* in the direction indicated by the **blue arrow**, continuing this motion until it reaches the opposite edge of the tray.

**Your task is to determine the sequence of occlusion events between the moving white candle and the stationary black candle throughout this planned trajectory.**

Select the option that best describes the temporal pattern of occlusion:

- (A) The two candles never occlude each other at any point.
- (B) One candle initially occludes the other, after which both remain visible.
- (C) Both candles are initially visible, then one occludes the other, and later both become visible again.
- (D) Both candles are initially visible, but one candle occludes the other at the end of the motion.

**Note:** "One occludes the other" means that at that moment either the white candle blocks the black candle, or the black candle blocks the white candle from the camera's viewpoint.

**GT: (C) Both candles are initially visible, then one occludes the other, and later both become visible again.**

Figure 11. Examples of planning tasks with occlusion reasoning in CausalSpatial.

## Collision Question Template Examples

### Description

"There is a {description} on the floor."  
 "You can see a {description} on the floor."  
 "In the picture, there is a {description} placed on the floor."  
 ....

### Level2 part 1

"is removing {object} sufficient to avoid all collisions?"  
 "will removing {object} ensure that there are no collisions?"  
 "is it enough to remove {object} to prevent all collisions?"  
 "by removing {object}, can we avoid all collisions?"  
 "will taking out {object} eliminate all collision risks?"  
 "is it true that removing {object} will prevent all collisions?"  
 ....

### Level2 part 2

If no, what else should be done to avoid all collisions?  
 If removing {object} is not enough, what else should be done to avoid all collisions?  
 If removing {object} does not prevent all collisions, what additional steps should be taken?  
 If removing {object} is insufficient, what else should be done to avoid all collisions?  
 ....

### Level1

"Is there any risk if it moves forward?"  
 "Will it collide with anything if it moves forward?"  
 "Is there a chance that it will hit something if it moves forward?"  
 "Could it collide with anything while moving forward?"  
 "Is there anything in the way if it moves forward?"  
 "Could it bump into something if it proceeds forward?"  
 "Is it risky for it to move forward?"  
 "Will it face any obstacles if it moves forward?"  
 "Is there a possibility that it could crash while moving forward?"  
 "Is it risky for it to move forward?"  
 "What should be done to avoid a collision?"  
 "How can we avoid a collision?"  
 "What action should be taken to prevent a collision?"  
 "How can a collision be avoided?"  
 "What measures should be taken to avoid a collision?"  
 "What action should be taken to avoid a collision?"  
 "To prevent a collision, what should be done?"  
 "Remove which object to avoid a collision?"  
 "Which object should be removed to avoid a collision?"  
 "Which object needs to be removed to avoid a collision?"  
 "To avoid a collision, which object should be removed?"  
 ....

Figure 12. Examples of collision question templates in CausalSpatial. Each question is composed by sampled object descriptions and a sampled question either from L1 or L2. The questions from L2 are composed by two parts, with each part sampled separately from "part1" and "part2" to ensure question diversity.

**Compatibility Question Template Examples**

## Level 1

If the **{falling object}** falls freely from its current position, can it fit into the **{container}**?  
 'Fit into' means it doesn't exceed the horizontal plane of the **{container}**'s opening.  
 Answer by (A) Yes, (B) No or (C) Not sure.

## Level 2

Now there is already a **{another object}** in the **{container}**. If the **{falling object}** falls freely from its current position, can it fit into the **{container}**?  
 'Fit into' means it doesn't exceed the horizontal plane of the **{container}**'s opening.  
 Answer by (A) Yes, (B) No or (C) Not sure.

**Physics Question Template Examples**

## Level1

Based on the **{ball}**'s trajectory shown in the image, will the **{ball}** go into the goal?  
 Note: The red box indicates the starting point of the trajectory.  
 Answer by (A) Not sure; (B) Yes; (C) No.

## Level2

If the **{balls}** moves in the direction of the red arrow, will any ball go into the pocket and score?  
 Note: Only consider direct shots and ball-to-ball collisions.  
 Answer by (A) Not sure; (B) Yes; (C) No.

Figure 13. Examples of Compatibility and Trajectory question templates in CausalSpatial.

**Occlusion Question Template Examples**

## Task Description

To achieve the required arrangement, you must predict the visual outcome of the following action.  
 To obtain the desired arrangement, you must predict the visual consequences of executing the following action.  
 To reach the target arrangement, you need to anticipate the visual outcome produced by the following action.  
 To achieve the desired configuration, you must predict the visual result of the action below.

## Level1 Template1

If the **{occluder object}** moves backward, can the **{occluded object}** **{location of the occluded object}** be removed from **{location of the occluded object}** without being blocked by the **{occluder object}**?  
 Answer by (A) Not sure; (B) Yes; (C) No.

## Level2 Template1

The red and blue arrows indicate the directions of two perpendicular edges of the **{platform}**.  
 There are four candles on the **{platform}**:**{obj1}**, **{obj2}**, **{obj3}**, **{obj4}**...

## Level1 Template2

If the **{occluder}** moves **{direction}** by the distance of one **{occluder}**, would the **{occluded object}** be revealed or occluded?  
 Note: All directions (left, right, forward, backward) are relative to the **{occluder}**'s own coordinate system, and the **{occluder}** moves straight along the direction by the length of one **{occluder}**.  
 Answer by (A) Revealed; (B) Not sure; (C) Occluded.

Now if the **{occluder}** moves along the edge of the tray in the direction of the blue arrow until it reaches the opposite edge, describe how the occlusion relationship between the **{occluder}** and the **{occluded object}**.

## Level1 Template3

The red and blue arrows indicate the directions of two perpendicular edges of the **{platform}**. Now the **{occluded object}** is occluded by the **{occluder}**.  
 If the **{occluded object}** moves in the opposite direction of the blue arrow, would the **{occluded object}** be fully revealed?  
 Answer by (A) Not sure; (B) Yes; (C) No.

Specify one of the following:  
 (A) initially both visible, then one occludes the other, then both visible again;  
 (B) initially both visible, then one occludes the other at the end;  
 (C) the two candles never occlude each other;  
 (D) initially one occludes the other, then both become visible;  
 (E) Not sure.

Figure 14. Examples of occlusion question templates in CausalSpatial. Each question is composed by a sampled task description and a sampled question either from L1 or L2. L1 has three different templates.